

---

---

# Modeling and Analysis of Active Full Vehicle Suspension Model Optimized Using the Advanced Fuzzy Logic Controller

**Shailendra Kumar and Amit Medhavi**

*Mechanical Engineering Department, Kamla Nehru Institute of Technology, Sultanpur, Uttar Pradesh—228118, India. E-mail: shailendra.kumar@knit.ac.in*

**Raghuvir Kumar**

*Director General at BN College of Engineering and Technology, Lucknow, Uttar Pradesh—226201, India.*

**P. K. Mall**

*Department of Mechanical Engineering, Babu Banarasi Das Engineering College, Lucknow, Uttar Pradesh—226010, India.*

(Received 11 August 2021; accepted 4 January 2022)

The suspension system plays a major role in automobiles to improve passenger comfort, passenger safety and road handling. It isolates the body of a vehicle from road disturbances. The full vehicle would be subjected to disturbances from all four wheels or a full suspension model of the vehicle and, thus, a full-suspension model of the vehicle should be added to the idea of an enhanced control preview. The input data for the fuzzy logic controller (FLC) is the velocity and acceleration of the front and rear wheels. Controller outputs are considered to be active forces that improve driver comfort, safety and road handling characteristics. The objective of this work is to model and analyse an active full vehicle suspension. The model is optimized using advanced FLC to improve driver comfort, safety and road handling. The mathematical model for the active full vehicle suspension model has been derived. The necessary background for the Simulink fuzzy logic and FLC has been presented. All the simulations are carried out using MATLAB/SIMULINK, a high-performance numeric computation and visualization software package. The fuzzy logic-controlled active values have been compared with ordinary passive simulated values for road profiles. The result of the simulation show that the designed advanced FLC has improved ride comfort by effectively reducing the vehicle body displacement. There is also an appreciable reduction in velocity and acceleration with no increase in suspension travel.

---

## 1. INTRODUCTION

The automotive industry is concentrating more on passenger safety and comfort as technology advances. The vehicle suspension system plays an important part in providing passengers with riding comfort by separating the cabin from various road disturbances. The suspension system is classified primarily into three groups: i) Semi-active suspension system (SASS) ii) Active suspension system (ASS) and iii) Passive suspension system (PSS). Traditional springs and dampers are used in the PSS to absorb road disturbances.<sup>1</sup> It also allows for a trade-off between the comfort of the passenger ride and the control of the vehicle on the road. The traditional spring and externally operated damper are used in the SASS. The damping coefficient of this form can be managed based on the chassis acceleration sensor inputs that calculate the vertical acceleration of the vehicle's body. In addition to traditional passive suspension systems, the ASS utilizes force actuator ( $F_a$ ) components in a closed-loop control system.<sup>2</sup> Based on the feedback from the various sensors associated with it, the  $F_a$  provides sufficient control force to the device. First, a vehicle model is required to regulate the suspension.<sup>3</sup> Researchers are currently

studying the quarter-vehicle model, half-vehicle model<sup>4-9</sup> and full-vehicle model suspension system used to construct the active suspension regulation rule.<sup>10,11</sup> The quarter vehicle suspension model has the simplest construction and the degree of freedom (DOF) is the full vehicle suspension model that can better explain the dynamics of the vehicle.<sup>11,12</sup> The half-vehicle suspension model is used to provide a balance between precision and effectiveness. The researchers suggested different control systems to boost the efficiency of the ASS.<sup>13</sup> The control strategy is one of the most important characteristics of active suspensions and many control strategies have been studied in the literature, such as adaptive filtered-x,<sup>14</sup> optimal control,<sup>8</sup> sliding mode control,<sup>15,16</sup> H-infinity control,<sup>17-19</sup> fuzzy logic control (FLC),<sup>20-25</sup> neural network control,<sup>26-28</sup> model-free fractional-order sliding mode control,<sup>29</sup> based backstepping fast terminal sliding mode control<sup>30</sup> and preview control.<sup>31-38</sup> The idea of preview information in vehicle suspensions was first proposed by bender,<sup>39</sup> suggesting that the use of preview information would effectively enhance the efficiency of vehicles. In the control approach, preview information on road disturbances is used before road disturbances operate on the vehicle body. This method will reduce the response time of

the controller and actuator, thereby enhancing the suspension performance.<sup>34,40</sup> It is possible to model the vehicle suspension system as a half vehicle four-degree of freedom and to evaluate the efficiency of the linear quadratic regulator (LQR) and fuzzy control systems.<sup>41,42</sup> For the half vehicle, four-degree of freedom suspension system model,<sup>43</sup> a proportional-integral sliding control system has been developed. On the half vehicle four-degree of freedom suspension models, the linear and FLC system performance was analyzed.<sup>44</sup> For the 2-DOF quarter vehicle suspension model, the fuzzy logic control system method was suggested and evaluated and a comparative analysis was performed with a linear quadratic gaussian (LQG) controller.<sup>5</sup> The researchers suggested to the ANFIS controller that the nonlinearity of the system should be controlled using data from the full vehicle active suspension model proportional integral derivative (PID) control system.<sup>45</sup> The half-vehicle four-degree of freedom suspension system has been developed with the LQR controller.<sup>46</sup> The ANFIS design was evaluated using the data-driven approach for half-vehicle six-degree of freedom suspension systems and its performance was compared with PSS.<sup>47</sup> The proportional integral derivative control method has been created and studied for quarter vehicle two-DOF suspension systems.<sup>46</sup> The design of the fuzzy quarter suspension control system has been addressed.<sup>15,48,49</sup> The development of the ANFIS for the SASS controller has been discussed.<sup>50</sup> The road profile can be simulated to measure the performance of the suspension system under different road conditions based on ISO 8608.<sup>51,52</sup> The model of the LQR control system was suggested for the active suspension system.<sup>42,48,53,54</sup> Fuzzy logic control rules optimization research has been discussed. A hybrid learning algorithm and the ANFIS architecture has been discussed.<sup>55</sup> The ANFIS and proportional integral derivative controllers were built and tested using LabVIEW software on an experimental active suspension setup.<sup>56</sup> The design, development and implementation of a proportional integral derivative controller for auto-tuning have been discussed.<sup>57</sup> Using the MATLAB proportional integral derivative auto-tuning tool,<sup>58</sup> the PID controller was designed for a two-degree of the freedom suspension system. The road profile classification model based on ANFIS was developed using semi-active suspension vehicles. An accurate model of the actual system needs a full vehicle model with 7-DOF. A full vehicle model of ASS is developed by considering seven degrees of freedom namely four vertical motions of the wheel, pitch, roll and heave motion of the vehicle body. A H infinity controller was introduced for the full vehicle model to suppress the effect of road disturbances and parameter uncertainty in actuator dynamics.<sup>17</sup> A preview controller for full vehicle model-based active suspension was introduced with two control approaches. The first controller optimizes the displacement of the actuator whereas the second controller controls the pitch, heave and roll motion of the vehicle body.<sup>59</sup> The complexity of the mathematical model of the full vehicle and the nonlinear behavior of the actuator has increased the difficulties of applying conventional control schemes to the active suspension system.<sup>21,60</sup> Hence a model-free controller based on intelligent control schemes like fuzzy logic, neural networks are gaining more importance in recent times and they are applied successfully to control suspension systems in real time.<sup>3,17,42</sup>

**Table 1.** Parameter values for full vehicle suspension.<sup>35</sup>

Parameter	Value
Mass of wheel (unsprung mass), $M_u$	59 kg
Mass of vehicle body (sprung mass), $M_s$	1500 kg
Tire spring stiffness, $K_u$	190000 N/m
Roll axis moment of inertia, $I_{xx}$	460 kg m <sup>2</sup>
Pitch axis moment of inertia, $I_{yy}$	2160 kg m <sup>2</sup>
Rear spring stiffness, $K_{sr}$	38000 N/m
Front spring stiffness, $K_{sf}$	35000 N/m
Distance between front of vehicle and C.G. of sprung mass, $a$	1.4 m
Distance between rear of vehicle and C.G. of sprung mass, $b$	1.7 m
C.G. height, $h_0$	0.508
Width of sprung mass, $w$	1.524 m
Distance between roll center and C.G., $h_{roll}$	0.3 m
Rear suspension damping, $C_{sr}$	1100 N s/m
Front suspension damping, $C_{sf}$	1000 N s/m

The researchers explored several control system techniques to improve the efficiency of the suspension model. This paper focused on the development and comparison of FLC for full vehicle model 7-DOF active suspension, providing insight into the design and selection of suitable control algorithms for vehicle suspension systems by other researchers. The reaction of these controls has been studied using the road profile, pitch, bumps, and rollover as road disturbances. Because of the benefits of the fuzzy control strategy and the effectiveness of the preview results, this study suggests using the wheelbase preview fuzzy control strategy to set up an active suspension control fuzzy preview to minimize chassis vibration to improve riding comfort. There is no current research that applies FLC system with preview information in the design of active full vehicle suspension system, according to the best knowledge of the authors.

## 2. MATHEMATICAL MODELING

The model of the system for the full-vehicle suspension system is given in Fig. 1. In contrast to the quarter-vehicle suspension model, the full-vehicle suspension model is a more sophisticated model that represented the precise dynamics of the vehicle's vertical motion. The full-vehicle suspension model is made up of a sprung mass and four unsprung masses linked to it at four corners via the suspension system's spring and damper. The study's model contained seven degrees of freedom, including the sprung mass's heave, roll, and pitch, as well as the vertical displacement of four unsprung masses.

The suspensions were modeled as spring components and linear viscous dampers between sprung mass and unsprung masses, whereas the tires were considered to be simple linear springs without viscous damping. It was also expected that the position of the sprung mass's center of gravity (CG) did not vary over time and that the suspension system's coordinate system is linked to the vehicle's CG and aligned with the vehicle's major axes. The small-angle approximation is employed to acquire the equations of motion, which added to the model's restriction.<sup>19</sup> The roll and pitch angles induced during the operation were considered to be small, and the small-angle approximation was utilized to obtain the equations of motion. Table 1 lists the parameters utilized in this study.

Mathematical description of the study's model was given as

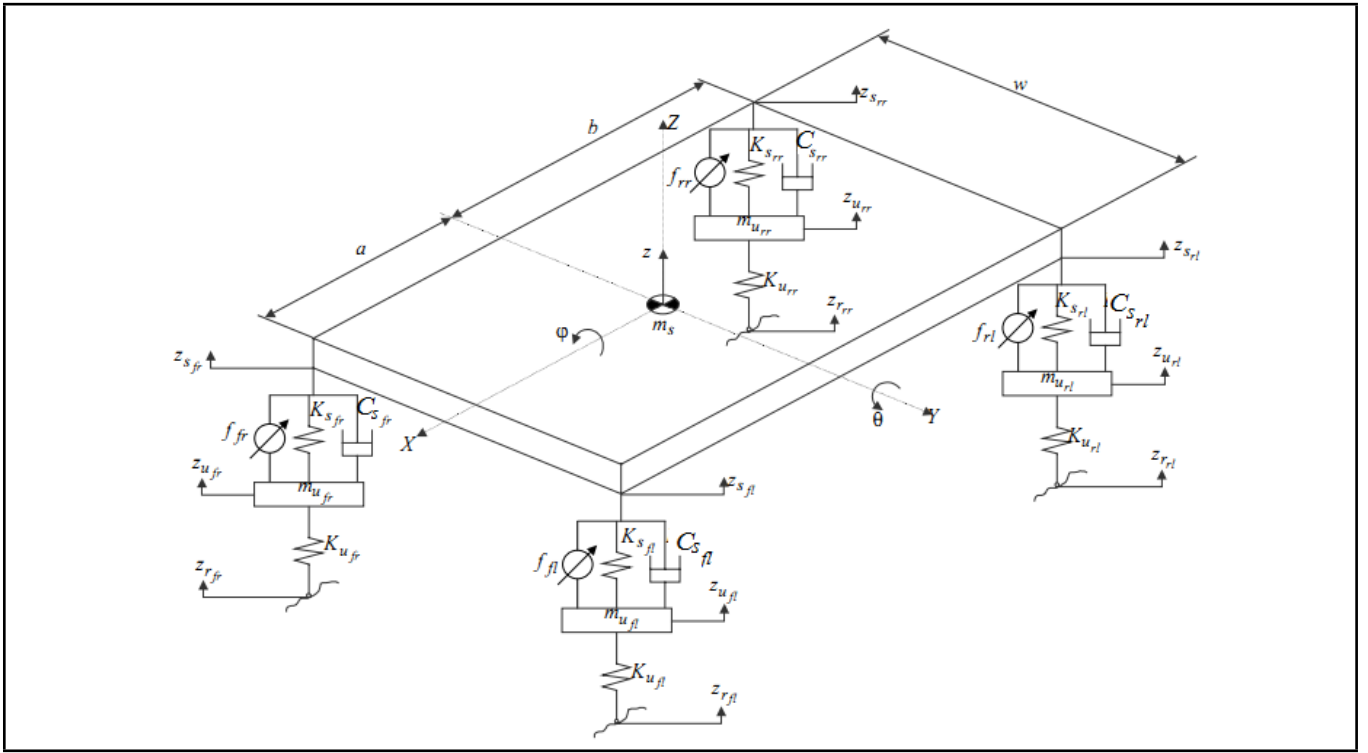


Figure 1. Active suspension model for full-vehicle system.

follows:

$$M_s \ddot{z} + (2C_{sf} + 2C_{sr}) \dot{z} - C_{sf} \dot{z}_{u_{fl}} - C_{sf} \dot{z}_{u_{fr}} - C_{sr} \dot{z}_{u_{rl}} - C_{sr} \dot{z}_{u_{rr}} + (2K_{sf} + 2K_{sr})z - K_{sf}z_{u_{fl}} - K_{sf}z_{u_{fr}} - K_{sr}z_{u_{rl}} - K_{sr}z_{u_{rr}} - (2aC_{sf} - 2bC_{sr})\dot{\theta} - (2aK_{sf} - 2bK_{sr})\theta - F_{fl} - F_{fr} - F_{rl} - F_{rr} = 0; \quad (1)$$

$$I_{yy} \ddot{\theta} + (2a^2C_{sf} - 2b^2C_{sr})\dot{\theta} + (2a^2K_{sf} - 2b^2K_{sr})\theta - (2aC_{sf} - 2bC_{sr})\dot{z} + aC_{sf}\dot{z}_{u_{fl}} + aC_{sf}\dot{z}_{u_{fr}} - bC_{sr}\dot{z}_{u_{rl}} - bC_{sr}\dot{z}_{u_{rr}} - (2aK_{sf} - 2bK_{sr})z + aK_{sf}z_{u_{fl}} + aK_{sf}z_{u_{fr}} - bK_{sr}z_{u_{rl}} - bK_{sr}z_{u_{rr}} + aF_{fl} + aF_{fr} - bF_{rl} - bF_{rr} = 0; \quad (2)$$

$$I_{xx} \ddot{\phi} + \frac{1}{4}w^2(2C_{sf} + 2C_{sr})\dot{\phi} + \frac{1}{4}w^2(2K_{sf} + 2K_{sr})\phi - \frac{1}{2}wC_{sf}\dot{z}_{u_{fl}} + \frac{1}{2}wC_{sf}\dot{z}_{u_{fr}} - \frac{1}{2}wC_{sr}\dot{z}_{u_{rl}} + \frac{1}{2}wC_{sr}\dot{z}_{u_{rr}} - \frac{1}{2}wK_{sf}z_{u_{fl}} + \frac{1}{2}wK_{sf}z_{u_{fr}} - \frac{1}{2}wK_{sr}z_{u_{rl}} + \frac{1}{2}wK_{sr}z_{u_{rr}} - \frac{1}{2}wF_{fl} + \frac{1}{2}wF_{fr} - \frac{1}{2}wF_{rl} + \frac{1}{2}wF_{rr} = 0; \quad (3)$$

$$M_u \ddot{z}_{u_{fl}} - C_{sf} \dot{z} + C_{sf} \dot{z}_{u_{fl}} + aC_{sf} \dot{\theta} + aK_{sf} \theta - \frac{1}{2}wC_{sf} \dot{\phi} - \frac{1}{2}wK_{sf} \phi + (K_{sf} + K_u)z_{u_{fl}} - K_{sf}z - K_u z_{r_{fl}} + F_{fl} = 0; \quad (4)$$

$$M_u \ddot{z}_{u_{fr}} - C_{sf} \dot{z} + C_{sf} \dot{z}_{u_{fr}} + aC_{sf} \dot{\theta} + aK_{sf} \theta + \frac{1}{2}wC_{sf} \dot{\phi} + \frac{1}{2}wK_{sf} \phi + (K_{sf} + K_u)z_{u_{fr}} - K_{sf}z + K_u z_{r_{fr}} + F_{fr} = 0; \quad (5)$$

$$M_u \ddot{z}_{u_{rl}} - C_{sr} \dot{z} + C_{sf} \dot{z}_{u_{rl}} - bC_{sr} \dot{\theta} - bK_{sr} \theta - \frac{1}{2}wC_{sr} \dot{\phi} - \frac{1}{2}wK_{sr} \phi + (K_{sr} + K_u)z_{u_{rl}} - K_{sr}z - K_u z_{r_{rl}} + F_{rl} = 0; \quad (6)$$

$$M_u \ddot{z}_{u_{rr}} - C_{sr} \dot{z} + C_{sf} \dot{z}_{u_{rr}} - bC_{sr} \dot{\theta} - bK_{sr} \theta + \frac{1}{2}wC_{sr} \dot{\phi} - \frac{1}{2}wK_{sr} \phi + (K_{sr} + K_u)z_{u_{rr}} - K_{sr}z - K_u z_{r_{rr}} + F_{rr} = 0; \quad (7)$$

$$F_c - \frac{MV^2}{R} = 0; \quad (8)$$

$M$ ,  $F_c$ , and  $V$  represents total vehicle mass, centripetal force, and vehicle speed, respectively.  $R$  is the road's radius of curvature. The car will rollover due to this centripetal force, which should be avoided. To evaluate the rollover dynamics in this investigation, an additional input to the vehicle was supplied in addition to the 4-wheel road input disturbances. To simulate driving on a curved road and incorporate rollover, the system model was given a centripetal force as an input. The equation gave the roll moment operating on the vehicle due to this centripetal force:

$$M_{roll} - F_c h_{roll} = 0; \quad (9)$$

where  $M_{roll}$  is the vehicle's rolling moment, and  $h_{roll}$  was the distance between the vehicle's center of gravity and the roll

center. The input of the rolling moment was applied to Eq. (3), and the resulting equation is provided by Eq. (10):

$$\begin{aligned}
 I_{xx}\ddot{\varphi} + \frac{1}{4}w^2(2C_{sf} + 2C_{sr})\dot{\varphi} + \frac{1}{4}w^2(2K_{sf} + 2K_{sr})\varphi - \\
 \frac{1}{2}wC_{sf}\dot{Z}_{ufl} - \frac{1}{2}wC_{sr}\dot{Z}_{url} + \frac{1}{2}wC_{sf}\dot{Z}_{ufr} + \\
 \frac{1}{2}wC_{sr}\dot{Z}_{urr} + \frac{1}{2}wK_{sf}Z_{ufr} - \frac{1}{2}wK_{sf}Z_{ufl} - \\
 \frac{1}{2}wK_{sr}Z_{url} + \frac{1}{2}wK_{sr}Z_{urr} - \frac{1}{2}wF_{fl} + \frac{1}{2}wF_{fr} - \\
 \frac{1}{2}wF_{rl} + \frac{1}{2}wF_{rr} - M_{roll} = 0; \tag{10}
 \end{aligned}$$

### 2.1. State Space Formulation of the Full Vehicle Model

The state-space variables for the full vehicle suspension model are assigned as in work of Senthilkumar et al.<sup>61</sup> Nomenclature:

- $y_1 = \dot{Z}$  velocity (payload speed of sprung mass)
- $y_2 = \dot{\theta}$  angular velocity
- $y_3 = \dot{\varphi}$  roll angular velocity
- $y_4 = \dot{Z}_{ufl}$  left-front wheel unsprung mass speed
- $y_5 = \dot{Z}_{ufr}$  right-front wheel unsprung mass speed
- $y_6 = \dot{Z}_{url}$  left-rear wheel unsprung mass speed
- $y_7 = \dot{Z}_{urr}$  right-rear wheel unsprung mass speed
- $y_8 = Z$  heave position (ride height of sprung mass)
- $y_9 = \theta$  pitch angle
- $y_{10} = \varphi$  roll angle
- $y_{11} = Z_{ufl}$  left-front wheel unsprung mass displacement
- $y_{12} = Z_{ufr}$  right-front wheel unsprung mass displacement
- $y_{13} = Z_{url}$  left-rear wheel unsprung mass displacement
- $y_{14} = Z_{urr}$  right-rear wheel unsprung mass displacement

The state-space equation is

$$\dot{\{y\}} = A\{y\} + B\{f\} + D\{r\}; \tag{11}$$

where

$\{y\} = [y_1, y_2, y_3, y_4, y_5, y_6, y_7, y_8, y_9, y_{10}, y_{11}, y_{12}, y_{13}, y_{14}]^T$  is the state vector;  $\{r\} = [Z_{rfl}, Z_{rfr}, Z_{rrl}, Z_{rrr}, M_{roll}]^T$  is the road disturbance input vector;  $\{f\} = [F_{fl}, F_{fr}, F_{rl}, F_{rr}]^T$  is the control force input vector;  $A$ ,  $B$ , and  $D$  are invariant coefficients.

### 3. FUZZY LOGIC CONTROLLER DESIGN

The FLC system provides an intuitive methodology to convert imprecise input into precise inputs. The FLC system normally involves 3 phases, i.e., fuzzification, control rule design and defuzzification. The conversion of real-number (crisp) input data to fuzzy data is involved in fuzzification. At this point, the membership functions (MF) used to fuzzy the suspension model input and output data are chosen. Next, by providing the IF-THEN control rules, the fuzzy inference system is built. The process of defuzzification transforms the output of the controller from fuzzy values into real values. FLC system can handle complexity, nonlinearity and unpredictable behavior of actuator dynamics in active suspension system.<sup>2,23,62,63</sup> The actual suspension travel of each wheel act as a control parameter for the fuzzy controller. Generally, the fuzzy logic control system consists of four parts, as shown in Fig. 2:

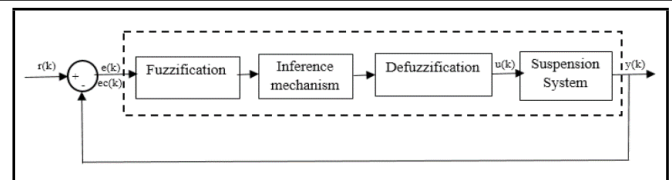


Figure 2. Fuzzy Controller Overall Layout.

- An interface for fuzzification that changes the inputs of the controller to linguistic variables that can be used in the inference mechanism. The fuzzy membership function can be described as follows:

$$K = \{(x, u_k(x)) \mid x \in K, u_k(x) \in [0, 1]\}; \tag{12}$$

where  $u_k(x)$  is the membership function specifying the grade of degree for any element in  $K$  which belongs to the fuzzy set  $K$ . The larger values of  $u_k(x)$  indicate the higher degrees of membership.

- A rule-based (RB), a set of linguistic (“if-then”) rules that store the information of how the mechanism can be managed. An inference process that produces the control judgment using the linguistic inputs and the RB.
- An interface for defuzzification, which transforms linguistic outputs into crisp ones. The centroid defuzzification technique can be expressed as:

$$Z_{COG} = \frac{\int_Z \mu_A(Z)Z dz}{\int_Z \mu_A(Z) dz}; \tag{13}$$

where  $Z_{COG}$  is the crisp output,  $\mu_A(Z)$  is the aggregated membership function and  $Z$  is the output variable.

- The fuzzification stage converts the  $e(k)$  error and  $ec(k)$  error change of suspension deflection into fuzzy values using the membership function. Fuzzy rules based on expert knowledge have been incorporated throughout the inference phase.

With five linguistic variables described in Fig. 3, the triangular membership functions. The actual input data is transformed into fuzzy values by this membership function. The traditional basis was the classical understanding of Mamdani. The range of the input variable and the output variable was calculated under different conditions by the results of the simulation. Table 2 shows the rules table for fuzzy logic control. The justification for the creation of the fuzzy control rules is to minimize the vertical displacement of the automobile body. There are two inputs to the fuzzy logic controller used in the active suspension: velocity, acceleration, and one output: the desired actuator force. For the five specified variables of the ASS defined by a fuzzy set, a possible choice of the membership functions is as follows.<sup>56</sup>

A two-dimensional fuzzy controller is constructed with two inputs and a single output. The basic input and output universes are determined by the measured passive suspension effects and by trial and error. There are  $[-0.3, 0.3]$ ,  $[-1.5, 1.5]$  and  $[-5000, 5000]$ , respectively in the simple universes of  $e$ ,  $ec$  and  $u$ . Three variables are differentiated between the MF of the input and output variables, i.e., NS: Negative Small; NB:

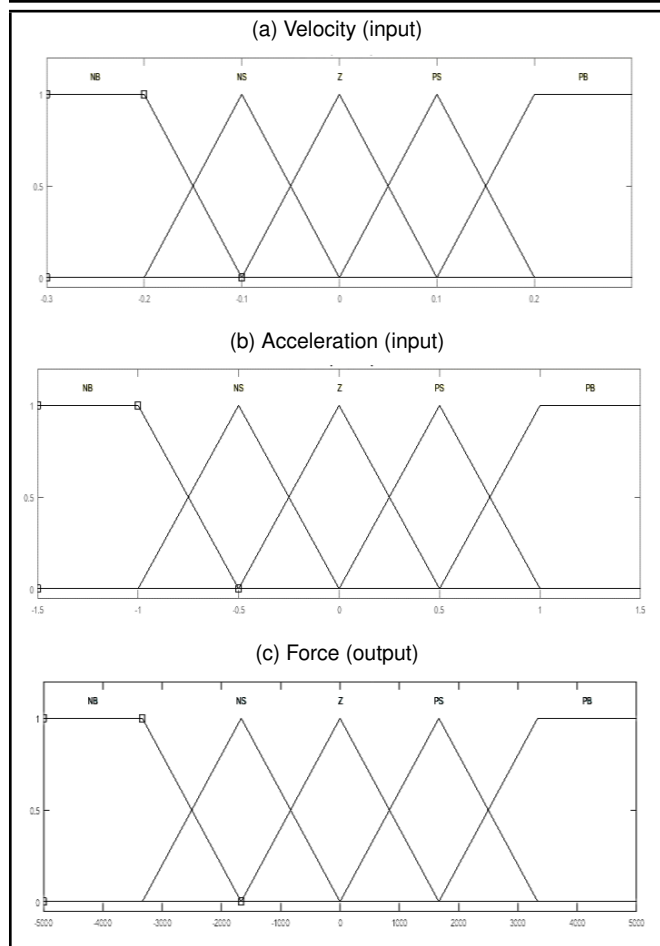


Figure 3. Membership function for input and output variables for fuzzy controller.

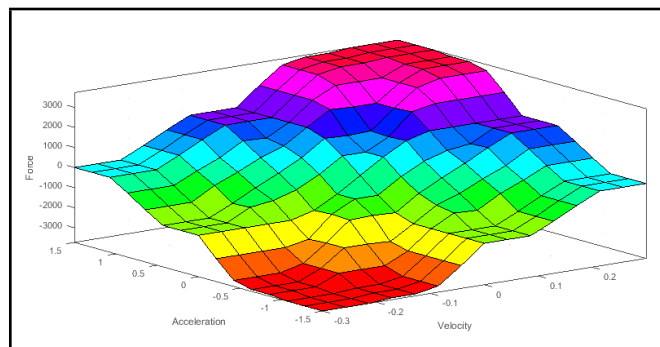


Figure 4. Fuzzy controller surface viewer.

Negative Big; Z: Zero; PB: Positive Big; PS: Positive Small;  $ec(k)$ : error change;  $e(k)$ : Error. Using the engineering context, the fuzzy rule base originally is given as follows: If (Velocity is NB) and (Acceleration is NB) then (Force is NB), If (Velocity is NB) and (Acceleration is NS) then (Force is NB) etc.

#### 4. ROAD PROFILE

Road profile irregularities have been categorized as being smooth, rough minor, or rough in nature. A smooth road profile signifies a road disturbance with a single bump. The rough minor and rough road profiles are characterized by uniform

Table 2. The rules table for fuzzy logic control.

$e / ec$	NB	NS	Z	PS	PB
NB	NB	NB	NS	NS	Z
NS	NB	NS	NS	Z	PS
Z	NS	NS	Z	PS	PS
PS	NS	Z	PS	PS	PB
PB	Z	PS	PS	PB	PB

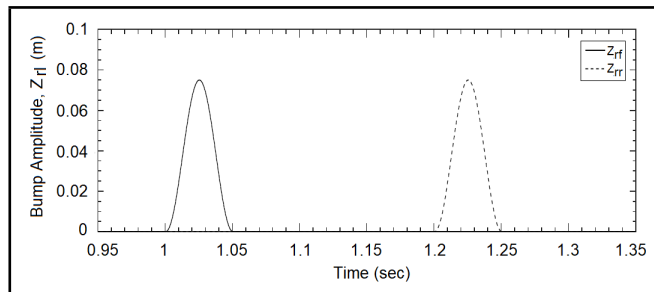


Figure 5. Bump road profile for the front and rear wheels.

bump height and non-uniform bump height, respectively:<sup>3</sup>

$$Z_{rf} = \begin{cases} \frac{a_0}{2} \left( 1 - \cos \left( \frac{2\pi V t_f}{\lambda_0} \right) \right) & 1 \leq t_f \leq 1 + \frac{\lambda_0}{V}; \\ 0 & \text{otherwise;} \end{cases} \quad (14)$$

$$Z_{rr} = \begin{cases} \frac{a_0}{2} \left( 1 - \cos \left( \frac{2\pi V t_r}{\lambda_0} \right) \right) & t_{r0} \leq t_r \leq t_{r0} + \frac{\lambda_0}{V}; \\ 0 & \text{otherwise.} \end{cases} \quad (15)$$

To investigate the behavior, two types of road input stimulation were used in this study: left wheel input and a speed breaker. The front-left and rear tires got a single bump for the left wheel input. Both or either of the front or rear tires contacted the bump for the speed breaker input. Figure 5 shows a graphical representation of the road profile. The road profile bump inputs for the rear wheel and front wheel were calculated using the formulae below. Where  $V$  is the vehicle forward velocity,  $\lambda_0$  is the disturbance wavelength,  $a_0$  is the bump amplitude,  $t$  is the simulation time and subscripts  $rr$  and  $rf$  denoted the road-rear and road-front wheel inputs to the suspension, respectively.  $t_{r0} = 1 + t_d$ , where  $t_d$  is the time delay between the rear wheel and front wheel, written as:

$$t_d = \frac{a + b}{V}; \quad (16)$$

where  $a$  is the distance between the vehicle's front and rear centers of gravity, and  $b$  is the distance between the vehicle's front and rear centers of gravity;  $a_0 = 0.075$  m,  $V = 15.50$  m/s, and  $\lambda_0 = 0.775$  m.

### 5. RESULT AND DISCUSSION

#### 5.1. Response of the Passive System

The reactions of the passive vehicle suspension system for the two inputs are compared. Figures 6 and 7 show that the amplitude of the response for the vehicle's vertical bounce and pitch motion is higher in the speed breaker input than in the left wheel input. Because both front-wheel tires contact the bump at the same time for the speed breaker input, the vertical height

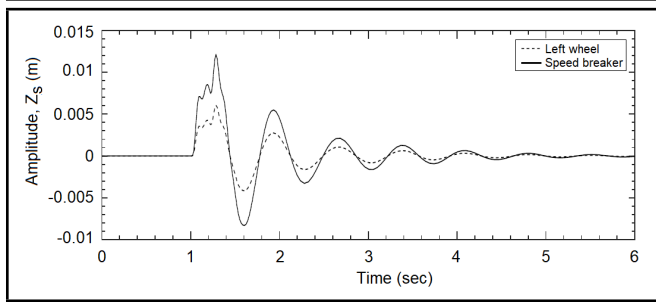


Figure 6. Vertical bounce with a passive suspension system.

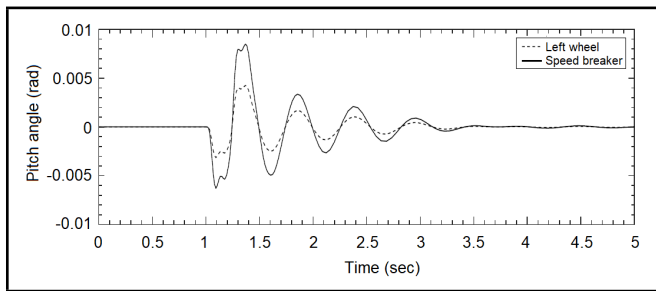


Figure 7. Pitching response with a passive suspension system.

and pitch angle are higher. Figure 8 illustrates that when a speed breaker is applied, there is no roll motion since both the front and rear suspension wheels contact the bump at the same time, but when the bump is delivered solely to the left wheels, the car is raised and a rolling motion is visible, as predicted.

Figure 9 depicts the response of the front and rear wheels in terms of vertical displacement. Because the rear suspension is more difficult, the vertical amplitude of motion of the rear wheel is greater than that of the front wheel. The wheel displacement plot is used to examine the contact between the tire and the road surface. When the road bump input is supplied exclusively to the left tires, Figs. 10 and 11 demonstrate the difference between the vertical motion of the wheels and the road irregularities for the front and rear suspensions. A positive number shows that there is a gap between the tire and the road surface, while a negative value indicates that the tire has been “bitten” by the road surface. The contact should be continuous and the difference should be as near to zero as possible for optimal vehicle control.

## 5.2. Body Attitude

Body bounce, pitch, and roll are the three primary attitudes of an automobile’s body that are crucial for ride comfort and safety. The vehicle’s vertical displacement (body bounce) is

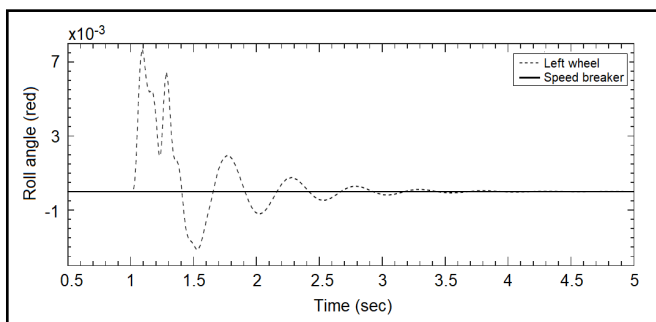


Figure 8. Rolling response with a passive suspension system.

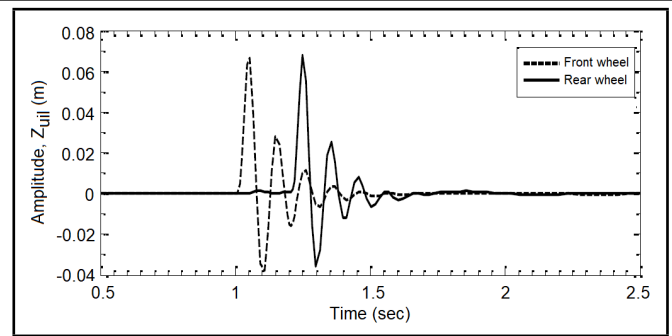


Figure 9. Vertical displacement of front and rear wheels.

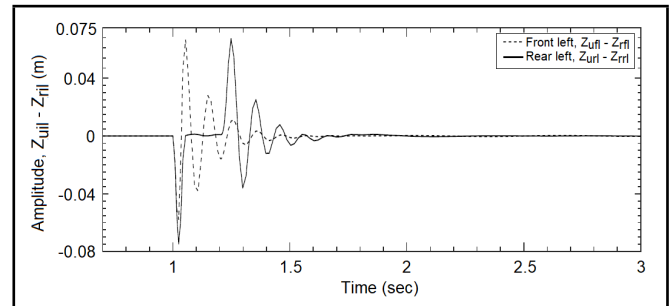


Figure 10. Vertical displacement of front and rear wheels.

reduced, resulting in an enhancement in ride comfort. Figure 12 shows the body bounce response; we can see that when the controller is applied, there is nearly 81% in vertical bounce and 60% in settling time of the passive response.

Pitching is one of the most uncomfortable body positions in a car, and it should be avoided if you want to be comfortable. Figure 13 depicts the suspension model’s pitching motion response. With the controller, the pitch angle of the passive suspension system is lowered by about 40%, and the settling time is cut by 50%.

Figure 14 depicts the rolling motion reaction. Roll is a very risky attitude that causes the majority of accidents when cornering or maneuvering. Rollover should be avoided at all costs by decreasing the roll angle to the smallest amount feasible. Based on the roll reaction, we can observe that there is a nearly 50% reduction in roll and an almost equal reduction in settling time. Based on the foregoing study, an active suspension system can significantly increase comfort and safety at high speeds.

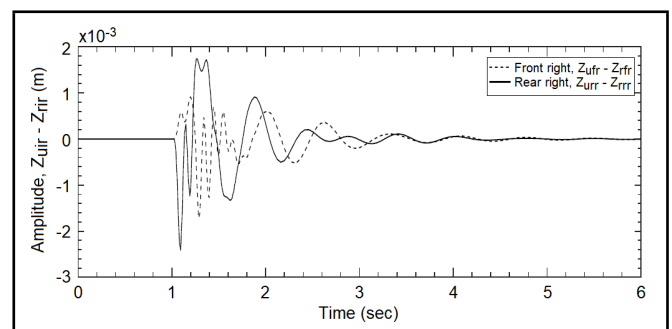


Figure 11. Vertical displacement of front and rear wheels.



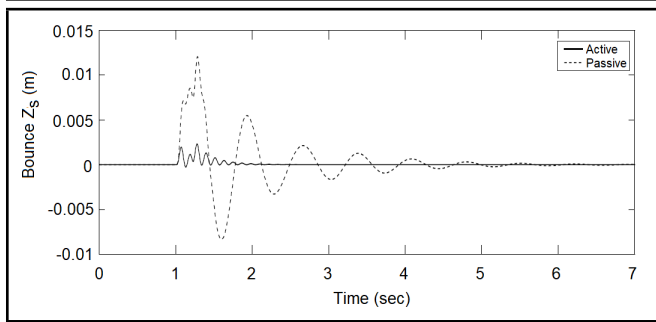


Figure 12. Vehicle body bounce vs. time.

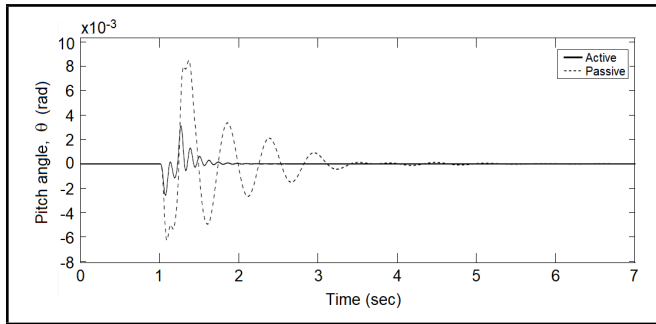


Figure 13. Vehicle body pitch angle vs. time.

### 5.3. Vertical Wheel Displacement

The tire-to-road-surface contact is evaluated using vertical wheel displacement. The decrease in overshoot in Fig. 15 indicates that the active system has enhanced tire-to-road surface contact. When the automobile hits a bump or cornering, the ASS should be built to prevent the car from skidding or drifting. A positive indication shows that there is a space between the tire and the road surface, while a negative sign indicates that the tire has been bitten by the road surface. Figure 15(a) depicts the vertical wheel displacement for the left wheel, whereas Fig. 15(b) depicts the vertical wheel displacement for the right wheel. The data show that the active suspension system improves surface contact between the tire and the road, resulting in a smoother ride.

### 5.4. Response to Cornering

Our research had been limited to straight road driving, rolling is a highly dangerous body position for a vehicle while cornering or maneuvering, and it is the cause of many road accidents. As a result, from a safety standpoint, this should be removed or reduced.

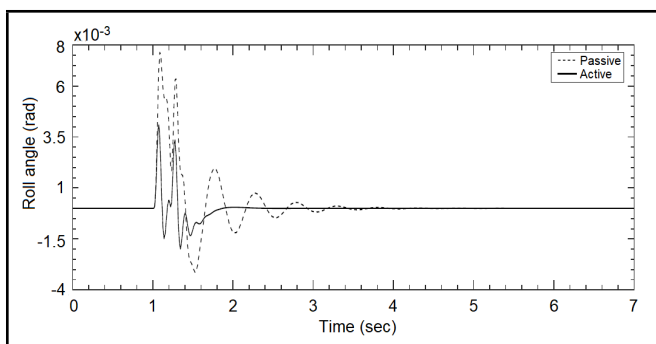


Figure 14. Vehicle body roll angle vs. time.

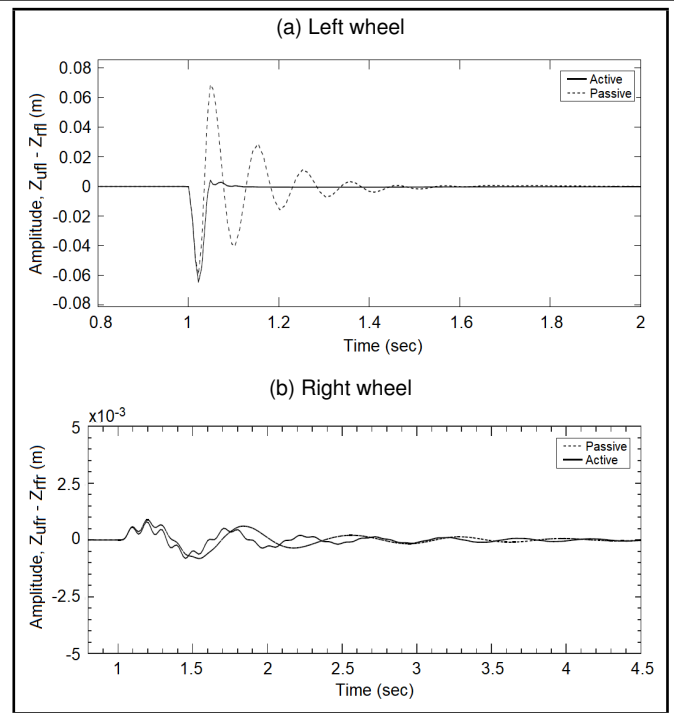


Figure 15. Vertical displacement of vehicle wheels vs. time.

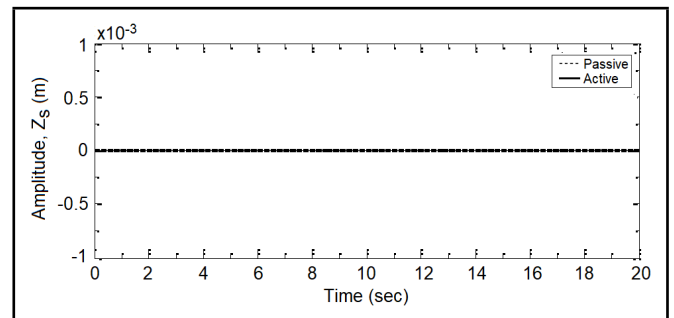


Figure 16. Vehicle body vertical amplitude vs. time during cornering.

The study uses a curving road with a radius of 40 meters and a vehicle speed of 25 meters per second as the road input. The length of the curved portion is such that the car enters the curved path in 2 seconds, travels 250 meters, and exits on the straight road in 2 seconds.

Figures 16 and 17(a) depict the vehicle's vertical displacement and pitching reaction, respectively. Because the car is traveling on a flat curving road, the active and passive reactions are almost identical, and the response is practically nil. The roll response of the active and PSS during cornering is seen in Fig. 17(b). The active system has a maximum roll angle of 0.00174533 rad (0.10°), which is virtually insignificant, but the PSS has a maximum roll angle of 0.1019 rad (5.84°). The roll angle has been reduced by about 98 percent, allowing the rollover to be avoided.

The vertical displacement of the left and right wheels with the passive and active suspension types is shown in Fig. 18(a) and (b). When the car turns to the left, the left wheel is raised a few millimeters, and there is no longer any contact between the left tires and the road, which is dangerous and should be avoided. The active suspension's response demonstrates that this issue has been resolved and that a greater tire-to-road grip has been obtained. The findings show that ASS is safer for

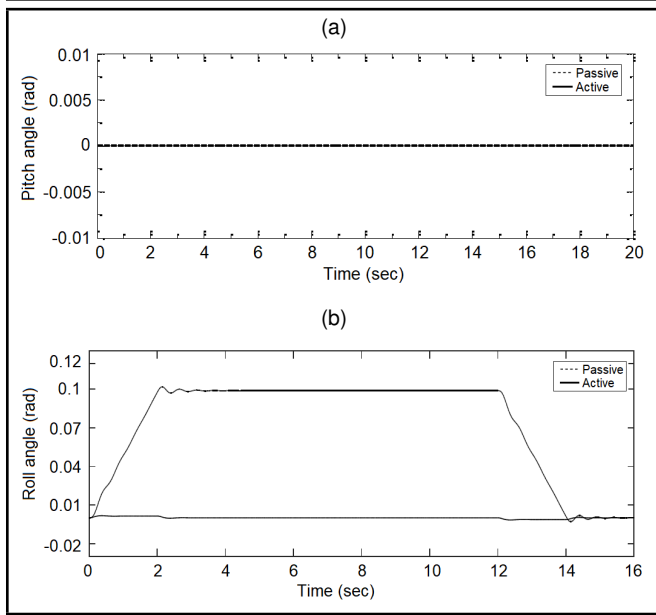


Figure 17. (a) Vehicle body pitch angle vs time, (b) Vehicle body roll angle vs. time, respectively during cornering.

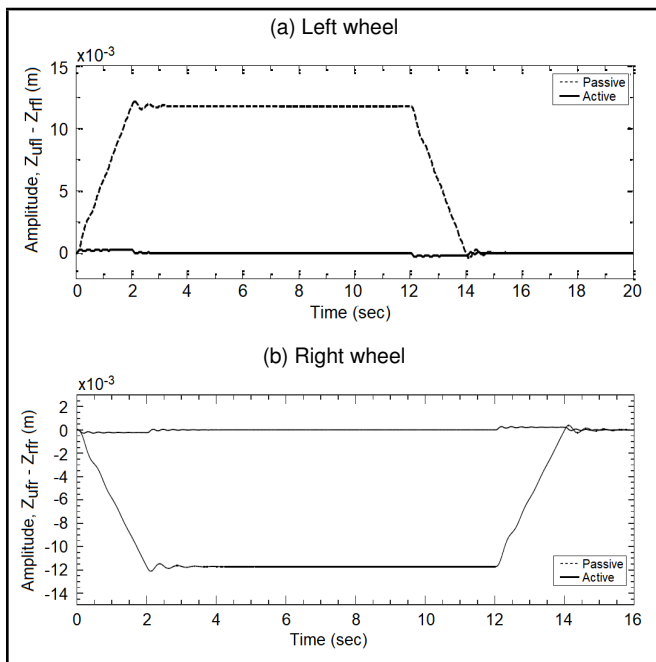


Figure 18. Vertical wheel Displacement vs. time during cornering.

rollover during turning and maneuvering, and is especially desired for high-speed cars.

### 5.5. Feed-Forward Control System

If the excitation is known ahead of time, the control signal can be delivered sooner to conduct the needed remedial action, according to the feed-forward control approach. When it comes to the vehicle suspension system, the road profile encountered by the front wheel will be the same as the disturbance experienced by the rear wheels, but with a time delay that is dependent on the vehicle's speed. The control signals applied to the front suspension are supplied after a time delay, which is determined by the controller's reaction time and the vehicle's speed, to regulate the rear suspension's disturbances.

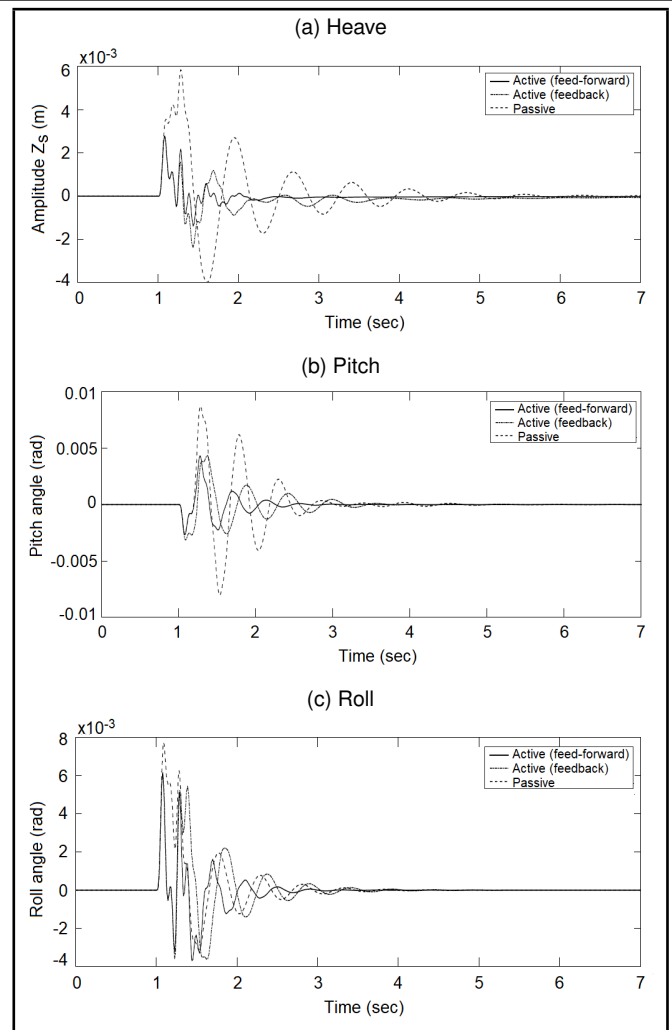


Figure 19. Response with the feed-forward system.

Figure 19 depicts the response with feed-forward control, which has a smaller amplitude but a longer settling time than the feedback response. This is undesirable because body mass, or spring-mass, connects the front and rear suspensions; when the front suspension is disturbed, the bodyweight is behind the suspension; when the rear suspension is disturbed, the bodyweight is in front, but the applied control, which is taken from the front suspension, assumes the body weight behind.

## 6. CONCLUSION

This study simulates the active suspension of a full vehicle model and develops a fuzzy logic controller for the suspension system. The study proposes a fuzzy-logic-controlled active suspension system for the passenger vehicle. The use of a fuzzy logic-based dynamic suspension controller improves ride comfort for cars traveling on varied road profiles while also reducing body acceleration. The reaction is investigated for disturbances such as road excitation and those generated by the vehicle itself. From the results obtained while investigating the performance of a vehicle running on a straight road and that subjected to bump disturbances, it has been found that when an active suspension system is used an 81% reduction in vertical amplitude is obtained while the settling time of the vertical disturbances due to the bump is reduced by 60%. Furthermore, it is evident from the results that the pitch angle is reduced by



40% followed by a reduction of 50% in settling time during pitching. A 50% reduction in roll angle as well as for settling time during rolling motion is achieved by the use of an active suspension system. The results obtained also help to conclude that a 98% reduction in roll angle is also achieved during the cornering of the vehicle. The current study shows that, during the simulation of an active suspension system with sensing and actuating constraints, the performances of components of the system have a significant impact on the results obtained. The controller should be tuned carefully, failing in which the overshoot of the system rises rapidly and affects the results. The simulation results showed that the suggested active suspension system is highly successful in isolating the vehicle body from vibrations.

## REFERENCES

- <sup>1</sup> Bhangal, N. S. and Raj, K. A. Fuzzy control of vehicle active suspension system, *International Journal of Mechanical Engineering and Robotics Research*, **5**, 144–148, (2016). <https://dx.doi.org/10.18178/ijmerr.5.2.144-148>
- <sup>2</sup> Sadeghi, M. S., Varzandian, S., and Barzegar, A. Optimization of classical PID and fuzzy PID controllers of a nonlinear quarter car suspension system using PSO algorithm, *1st International eConference on Computer and Knowledge Engineering*, 172–176, (2011). <https://dx.doi.org/10.1109/ICCCKE.2011.6413346>
- <sup>3</sup> Gandhi, P., Adarsh, S., and Ramachandran, K. I. Performance analysis of half car suspension model with 4 DOF using PID, LQR, FUZZY and ANFIS controllers, *Procedia Computer Science*, **115**, 2–13, (2017). <https://dx.doi.org/10.1016/j.procs.2017.09.070>
- <sup>4</sup> Yoshimura, T., Kume, A., Kurimoto, M., and Hino, J. Construction of an active suspension system of a quarter car model using the concept of sliding mode control, *Journal of Sound and Vibration*, **239**, 187–199, (2001). <https://dx.doi.org/10.1006/jsvi.2000.3117>
- <sup>5</sup> Gururaj, M. S. and Selvakumar, A. A. Fuzzy logic control for half car suspension system using MATLAB, *International Journal of Engineering Research & Technology (IJERT)*, **3**, 10–16, (2014).
- <sup>6</sup> Kunya, A. B. and Ata, A. A. Half car suspension system integrated with PID controller, *Proc. of the 29th European Conference on Modelling and Simulation, ECMS 2015*, **8**, 233–238, (2015). <https://dx.doi.org/10.7148/2015-0233>
- <sup>7</sup> Mouleeswaran, S. Design and Development of PID Controller-Based Active Suspension System for Automobiles, In *PID Controller Design Approaches — Theory, Tuning and Application to Frontier Areas*, 71–98, (2012). <https://dx.doi.org/10.5772/2628>
- <sup>8</sup> Wu, S.-J., Chiang, H.-H., Chen, J.-H., and Lee, T.-T. Optimal fuzzy control design for half-car active suspension systems, *IEEE International Conference on Networking, Sensing and Control*, 583–588, (2004). <https://dx.doi.org/10.1109/ICNSC.2004.1297504>
- <sup>9</sup> Mustafa, G. I. Y., Wang, H., and Tian, Y. Model-free adaptive fuzzy logic control for a half-car active suspension system, *Studies in Informatics and Control*, **28**, 13–24 (2019). <https://dx.doi.org/10.24846/v28i1y201902>
- <sup>10</sup> Kumar, S., Medhavi, A., and Kumar, R. Modeling of an active suspension system with different suspension parameters for full vehicle, *Indian Journal of Engineering & Materials Science*, **28**, 55–63, (2021).
- <sup>11</sup> Kumar, S., Medhavi, A., and Kumar, R. Active and passive suspension system performance under random road profile excitations, *International Journal of Acoustics and Vibration*, **25**, 532–541, (2021). <https://dx.doi.org/10.20855/ijav.2020.25.41702>
- <sup>12</sup> Sharma, S. K., Pare, V., Chouksey, M., and Rawal, B. R. Numerical Studies Using Full Car Model for Combined Primary and Cabin Suspension, *Procedia Technology*, **23**, 171–178, (2016). <https://dx.doi.org/10.1016/j.protcy.2016.03.014>
- <sup>13</sup> Guclu, R. and Gulez, K. Neural network control of seat vibrations of a non-linear full vehicle model using PMSM, *Mathematical and Computer Modelling*, **47**, 1356–1371, (2008). <https://dx.doi.org/10.1016/j.mcm.2007.08.013>
- <sup>14</sup> Gan, Z., Hillis, A. J., and Darling, J. Adaptive control of an active seat for occupant vibration reduction, *Journal of Sound and Vibration*, **349**, 39–55, (2015). <https://dx.doi.org/10.1016/j.jsv.2015.03.050>
- <sup>15</sup> Yagiz, N., Hacıoglu, Y., and Taskin, Y. Fuzzy sliding-mode control of active suspensions, *IEEE Transactions on Industrial Electronics*, **55**, 3883–3890, (2008). <https://dx.doi.org/10.1109/TIE.2008.924912>
- <sup>16</sup> Yagiz, N., Yuksek, I., and Sivrioglu, S. Robust control of active suspensions for a full vehicle model using sliding mode control, *JSME International Journal Series C*, **43**, 253–258, (2000). <https://dx.doi.org/10.1299/jsmec.43.253>
- <sup>17</sup> Park, J. and Kim, Y. S. An H-infinity controller for active suspensions and its robustness based on a full-car model, *Proc. of the 14th IFAC World Congress*, 503–508, (1999).
- <sup>18</sup> Ning, D., Sun, S., Li, H., Du, H., and Li, W. Active control of an innovative seat suspension system with acceleration measurement based friction estimation, *Journal of Sound and Vibration*, **384**, 28–44, (2016). <https://dx.doi.org/10.1016/j.jsv.2016.08.010>
- <sup>19</sup> Kruczek, A., Stribrsky, A., Hyniova, K. H-infinity controlled actuators in automotive active suspension system, *Proc. of the 9th Biennial ASME Conference on Engineering Systems Design and Analysis ESDA08*, 1–5, (2008).
- <sup>20</sup> Rao, M. V. C. and Prahlad, V. A tunable fuzzy logic controller for vehicle-active suspension systems, *Fuzzy Sets and Systems*, **85**, 11–21, (1997). [https://dx.doi.org/10.1016/0165-0114\(95\)00369-X](https://dx.doi.org/10.1016/0165-0114(95)00369-X)

- <sup>21</sup> Guclu, R. Fuzzy logic control of seat vibrations of a non-linear full vehicle model, *Nonlinear Dynamics*, **40**, 21–34 (2005). <https://dx.doi.org/10.1007/s11071-005-3815-7>
- <sup>22</sup> Hurel, J., Mandow, A., and Garcia-Cerezo, A. Tuning a fuzzy controller by particle swarm optimization for an active suspension system, *Proc. of the 38th Annual Conference on IEEE Industrial Electronics Society IECON 2012*, 2524–2529, (2012). <https://dx.doi.org/10.1109/IECON.2012.6388697>
- <sup>23</sup> Moon, S. Y. and Kwon, W. H. Genetic-based fuzzy control for half-car active suspension systems, *International Journal of Systems Science*, **29**, 699–710, (1998). <https://dx.doi.org/10.1080/00207729808929564>
- <sup>24</sup> Sharkawy, A. B. Fuzzy and adaptive fuzzy control for the automobiles' active suspension system, *Vehicle System Dynamics*, **43**, 795–806, (2005). <https://dx.doi.org/10.1080/00423110500097783>
- <sup>25</sup> Taskin, Y., Hacioglu, Y., and Yagiz, N. The use of fuzzy-logic control to improve the ride comfort of vehicles, *Strojnicki Vestnik—Journal of Mechanical Engineering*, **53** (4), 233–240, (2007).
- <sup>26</sup> Taskin, Y., Hacioglu, Y. and Yagiz, N. Experimental evaluation of a fuzzy logic controller on a quarter car test rig, *Journal of the Brazilian Society of Mechanical Sciences and Engineering*, **39**, 2433–2445, (2017). <https://dx.doi.org/10.1007/s40430-016-0637-0>
- <sup>27</sup> Eslaminasab, N., Biglarbegan, M., Melek, W. W., and Golnaraghi, M. F. A neural network based fuzzy control approach to improve ride comfort and road handling of heavy vehicles using semi-active dampers, *International Journal of Heavy Vehicle Systems*, **14**, 135–157, (2007). <https://dx.doi.org/10.1504/IJHVS.2007.013259>
- <sup>28</sup> Eski, I. and Yildirim, S. Vibration control of vehicle active suspension system using a new robust neural network control system, *Simulation Modelling Practice and Theory*, **17**, 778–793, (2009). <https://dx.doi.org/10.1016/j.simpat.2009.01.004>
- <sup>29</sup> Wang, H. P., Mustafa, G. I. Y., and Tian, Y. Model-free fractional-order sliding mode control for an active vehicle suspension system, *Advances in Engineering Software*, **115**, 452–461, (2018). <https://dx.doi.org/10.1016/j.advengsoft.2017.11.001>
- <sup>30</sup> Wang, H., Chang, L., and Tian, Y. Extended state observer-based backstepping fast terminal sliding mode control for active suspension vibration, *Journal of Vibration and Control*, **27**, 2303–2318, (2021). <https://dx.doi.org/10.1177/1077546320959521>
- <sup>31</sup> Akbari, A., Koch, G., Pellegrini, E., Spirk, S., and Lohmann, B. Multi-objective preview control of active vehicle suspensions: Experimental results, *Proc. of the 2nd IEEE International Conference on Advanced Computer Control, ICACC 2010*, **3**, 497–502, (2010). <https://dx.doi.org/10.1109/ICACC.2010.5486804>
- <sup>32</sup> Elmadany, M. M., Abduljabbar, Z., and Foda, M. Optimal preview control of active suspensions with integral constraint, *Journal of Vibration and Control*, **9**, 1377–1400, (2003). <https://dx.doi.org/10.1177/1077546304031167>
- <sup>33</sup> Elmadany, M. M., Al Bassam, B. A., and Fayed, A. A. Preview control of slow-active suspension systems, *Journal of Vibration and Control*, **17**, 245–258, (2011). <https://dx.doi.org/10.1177/1077546310362451>
- <sup>34</sup> ElMadany, M. M. Control and evaluation of slow-active suspensions with preview for a full car, *Mathematical Problems in Engineering*, **2012**, (2012). <https://dx.doi.org/10.1155/2012/375080>
- <sup>35</sup> Hac, A. Optimal linear preview control of active vehicle suspension, *Vehicle System Dynamics*, **21**, 167–195, (1992). <https://dx.doi.org/10.1080/00423119208969008>
- <sup>36</sup> Nagiri, S., Doi, S., Shoh-No, S. I., and Hiraiwa, N. Improvement of ride comfort by preview vehicle-suspension system, SAE Technical Paper 920277, (1992). <https://dx.doi.org/10.4271/920277>
- <sup>37</sup> Kitching, K. J., Cebon, D., and Cole, D. J. An experimental investigation of preview control, *Vehicle System Dynamics*, **32**, 459–478, (1999). <https://dx.doi.org/10.1076/vesd.32.6.459.4226>
- <sup>38</sup> Li, P., Lam, J., and Cheung, K. C. Multi-objective control for active vehicle suspension with wheelbase preview, *Journal of Sound and Vibration*, **333**, 5269–5282, (2014). <https://dx.doi.org/10.1016/j.jsv.2014.06.017>
- <sup>39</sup> Tomizuka, M. Optimum linear preview control with application to vehicle suspension—Revisited, *Journal of Dynamic Systems, Measurement, and Control*, **98**, 309–315, (1976). <https://dx.doi.org/10.1115/1.3427040>
- <sup>40</sup> Arunachalam, K., Jawahar, P. M., and Tamilporai, P. Active suspension system with preview control—A review, SAE Technical Paper 2003-28-0037, (2003). <https://dx.doi.org/10.4271/2003-28-0037>
- <sup>41</sup> Hasbullah, F. and Faris, W. F. A comparative analysis of LQR and fuzzy logic controller for active suspension using half car model, *Proc. of the 2010 11th International Conference on Control Automation Robotics & Vision*, 2415–2420, (2010). <https://dx.doi.org/10.1109/ICARCV.2010.5707260>
- <sup>42</sup> Kumar, M. S. and Vijayarangan, S. Linear quadratic regulator controller design for active suspension system subjected to random road surfaces, *Journal of Scientific and Industrial Research*, **65**, 213–226, (2006).
- <sup>43</sup> Sam, Y. M. and Bin Osman, J. H. S. Modeling and control of the active suspension system using proportional integral sliding mode approach, *Asian Journal of Control*, **7**, 91–98, (2008). <https://dx.doi.org/10.1111/j.1934-6093.2005.tb00378.x>

- <sup>44</sup> Yoshimura, T., Nakaminami, K., Kurimoto, M., and Hino, J. Active suspension of passenger cars using linear and fuzzy-logic controls, *Control Engineering Practice*, **7**, 41–47, (1999). [https://dx.doi.org/10.1016/S0967-0661\(98\)00145-2](https://dx.doi.org/10.1016/S0967-0661(98)00145-2)
- <sup>45</sup> Senthil Kumar, P., Sivakumar, K., Kanagarajan, R., and Kuberan, S. Adaptive neuro fuzzy inference system control of active suspension system with actuator dynamics, *Journal of Vibroengineering*, **20**, 541–549, (2018). <https://dx.doi.org/10.21595/jve.2017.18379>
- <sup>46</sup> Mouleeswaran, S. Design and development of PID controller-based active suspension system for automobiles, *PID Controller Design Approaches—Theory, Tuning and Application to Frontier Areas*, ed. Dr. Marialena Vagia, IntechOpen, London, (2012). <https://dx.doi.org/10.5772/32611>
- <sup>47</sup> Zhang, G., Ye, S., Zhang, X., and Peng, J. The research of automobile suspension system performance based on the fuzzy neural network control, *Proc. of the 2014 IEEE Conference and Expo Transportation Electrification Asia-Pacific (ITEC Asia-Pacific)*, 1–6, (2014). <https://dx.doi.org/10.1109/ITEC-AP.2014.6941138>
- <sup>48</sup> Shirdel, A. H., Gatavi, E., and Hashemiyani, Z. Comparison of  $H_\infty$  and optimized-LQR controller in active suspension system, *Proc. of the 2nd International Conference on Computational Intelligence, Modelling and Simulation, CIMSIm 2010*, 241–246, (2010). <https://dx.doi.org/10.1109/CIMSIm.2010.42>
- <sup>49</sup> Foda, S. G. Fuzzy control of a quarter-car suspension system, *Proc. of the 12th International Conference on Microelectronics*, 231–234, (2000). <https://dx.doi.org/10.1109/ICM.2000.916451>
- <sup>50</sup> Nugroho, P. W., Du, H., Li, W., and Alici, G. Implementation of Adaptive Neuro Fuzzy Inference System controller on magneto rheological damper suspension, *Proc. of the 2013 IEEE/ASME International Conference on Advanced Intelligent Mechatronics*, 1399–1403, (2013). <https://dx.doi.org/10.1109/AIM.2013.6584290>
- <sup>51</sup> Dharankar, C. S., Hada, M. K., and Chandel, S. Numerical generation of road profile through spectral description for simulation of vehicle suspension, *Journal of the Brazilian Society of Mechanical Sciences and Engineering*, **39**, 1957–1967, (2017). <https://dx.doi.org/10.1007/s40430-016-0615-6>
- <sup>52</sup> Agostinacchio, M., Ciampa, D., and Olita, S. The vibrations induced by surface irregularities in road pavements—a Matlab® approach, *European Transport Research Review*, **6**, 267–275, (2014). <https://dx.doi.org/10.1007/s12544-013-0127-8>
- <sup>53</sup> Nagarkar, M. P. and Vikhe Patil, G. J. Performance analysis of quarter car active suspension system: LQR and  $H_\infty$  control strategies, *Proc. of the Third International Conference on Computing, Communication and Networking Technologies (ICCCNT'12)*, (2012). <https://dx.doi.org/10.1109/ICCCNT.2012.6396067>
- <sup>54</sup> Kaleemullah, M., Faris, W. F., and Hasbullah, F. Design of robust  $H_\infty$ , fuzzy and LQR controller for active suspension of a quarter car model, *Proc. of the 4th International Conference on Mechatronics (ICOM)*, 17–19, (2011). <https://dx.doi.org/10.1109/ICOM.2011.5937197>
- <sup>55</sup> Alhasa, W. and Suparta, K. M. *Modeling of Tropospheric Delays Using ANFIS*, Springer, Cham, (2016). <https://dx.doi.org/10.1007/978-3-319-28437-8>
- <sup>56</sup> Hari, V. M., Lakshmi, P., and Kalaivani, R. Design and implementation of adaptive neuro fuzzy inference system for an experimental active suspension system, *Proc. of the International Conference on Robotics, Automation, Control and Embedded Systems, RACE 2015*, 18–21, (2015). <https://dx.doi.org/10.1109/RACE.2015.7097272>
- <sup>57</sup> Sukede, A. K. and Arora, J. Auto tuning of PID controller, *Proc. of the 2015 International Conference on Industrial Instrumentation and Control (ICIC)*, 1459–1462, (2015). <https://dx.doi.org/10.1109/IIC.2015.7150979>
- <sup>58</sup> Ignatius, O. I., Obinabo, C. E., and Evbogbai, M. J. E. Modeling, design and simulation of active suspension system PID controller using automated tuning technique, *Network and Complex Systems*, **6**, 11–15, (2016).
- <sup>59</sup> Shuttlewood, D. W., Crolla, D. A., Sharp, R. S., and Crawford, I. L. Active roll control for passenger cars, *Vehicle System Dynamics*, **22**, 383–396, (1993). <https://dx.doi.org/10.1080/00423119308969038>
- <sup>60</sup> Kumar, S., Medhavi, A., and Kumar, R. Optimization of nonlinear passive suspension system to minimize road damage for heavy goods vehicle, *International Journal of Acoustics and Vibration*, **26**, 56–63, (2021). <https://dx.doi.org/10.20855/ijav.2020.25.11724>
- <sup>61</sup> Senthilkumar, P., Sivakumar, K., Kanagarajan, R., and Kuberan, S. Fuzzy control of active suspension system using full car model, *Mechanika: Dynamics of Mechanical Systems*, **24**, 240–247, (2018). <https://dx.doi.org/10.5755/j01.mech.24.2.17457>
- <sup>62</sup> Shao, X., Zhang, N. and Wang, L. Fuzzy control of hydraulically interconnected suspension with configuration switching, *Proc. of the 2013 IEEE International Conference on Vehicular Electronics and Safety*, 66–71, (2013). <https://dx.doi.org/10.1109/ICVES.2013.6619605>
- <sup>63</sup> Divekar, A. A. and Mahajan, B. D. Analytical Modeling and Self-tuned Fuzzy-PID Logic based Control for Quarter Car Suspension System using Simulink, *Proc. of the 2016 IEEE International Conference on Recent Trends in Electronics, Information and Communication Technology (RTEICT)*, 267–271, (2016). <https://dx.doi.org/10.1109/RTEICT.2016.7807825>